Electric field-gradient contributions to the chemical shifts of liquid water

Thomas M. Nymand
Department of Chemistry, Aarhus University, DK-8000 Århus C, Denmark

Per-Olof Åstrand
Chemical Laboratory III, H. C. Ørsted Institute, University of Copenhagen, DK-2100 København Ø, Denmark

(Received 11 February 1997; accepted 20 February 1997)

Contributions to the gas-to-liquid chemical shifts of water arising from the electric field gradient of the surrounding molecules have been calculated as a function of the temperature. Since the theoretical model is based on perturbation theory, this part of the chemical shift may be calculated from quadrupole shielding polarizabilities and statistical mechanical ensemble averages of external electric field-gradients. The contributions from the electric field gradients are found to be substantial and are calculated to −9.7 ppm for the oxygen shift and 0.7 ppm for the proton shift at room temperature. © *1997 American Institute of Physics.* [S0021-9606(97)01320-2]

I. INTRODUCTION

It has been established that intermolecular interactions as well as the interaction of a molecule with an external magnetic field can be described by perturbation theory.[1–4] Consequently, the calculation of chemical shifts in solutions may be partitioned into two parts:

(i) Quantum chemical calculations of derivatives of nuclear shieldings with respect to external perturbations such as electric fields, electric field gradients and geometric distortions. Note that these calculations are carried out for the isolated molecule.

(ii) Statistical mechanical ensemble averages of the magnitude of the perturbation, which may be obtained from molecular dynamics or Monte Carlo simulations of liquids and solutions. For obtaining accurate estimates of the electric field and its gradient, a proper description of the charge distribution of each molecule is required in the intermolecular potential.

The accuracy of the adopted intermolecular potential is thus crucial for modeling chemical shifts adequately. This has been demonstrated in the calculation of the gas-to-liquid oxygen shift of water by sampling water pentamers from molecular dynamics simulations of liquid water and calculating the shielding of the central water molecule.[5,6] For different water potentials, oxygen shifts in the range of −47 to −20 ppm have been obtained, demonstrating how sensitive the oxygen shift is with respect to the simulation potential.

The construction of intermolecular potentials using perturbation theory has been implemented in the NEMO approach.[7–9] Here it is important to note that many empirical force fields fit the Coulombic term of the interaction potential to experimental data—a procedure which does not attempt to reproduce the molecular dipole and quadrupole moments. These potentials are therefore not suitable for calculating ensemble averages of electric fields and electric field gradients. The electrostatics of a NEMO potential is represented with atomic charges, dipole moments and polarizability tensors reproducing the corresponding molecular properties and the response to an external electric field. Along with shielding polarizabilities, the NEMO method thus presents a consistent approach to obtain the properties needed for calculating chemical shifts of large molecules in solution based on first principle methods.

A reasonable starting point in the investigation of solvent effects on nuclear shieldings is the consideration of the gas-to-liquid shift of the most common solvent, liquid water. This approach has previously enabled us to calculate the proton shift and its temperature dependence in quantitative agreement with experiment,[10] by regarding electric-field and van der Waals contributions as well as a contribution arising from the different geometries of the water molecule in the gas phase and in the liquid. The oxygen shift, however, was not as well described, which may be due to that higher order contributions were lacking. Here, the method is therefore extended to the inclusion of electric field-gradient contributions to the shift, because it has been argued that this effect may be substantial for carbon and oxygen shieldings.[11–13] Field-gradient contributions should, however, be less substantial for the proton shielding since the electron structure at a hydrogen atom is mainly of *s*-character.

In the perturbation approach, the electrostatic part of the shift is expanded in terms of the properties describing the electrostatic interactions (using the Einstein summation convention)[3,11]

$$\sigma_{E,\alpha\beta} = \sigma'_{\alpha\beta,\gamma} E_\gamma + \frac{1}{2}\sigma''_{\alpha\beta,\gamma,\delta} E_\delta E_\gamma + \cdots + \sigma'_{\alpha\beta,\gamma\delta} E_{\gamma\delta} + \frac{1}{2}\sigma''_{\alpha\beta,\gamma\delta,\epsilon\sigma} E_{\epsilon\sigma} E_{\gamma\delta} + \cdots, \tag{1}$$

where E_γ and $E_{\gamma\delta}$ denote components of the electric field and the electric field-gradient, respectively, both at the nucleus. $\sigma'_{\alpha\beta,\gamma}$ and $\sigma''_{\alpha\beta,\gamma,\delta}$ are components of the dipole shielding polarizability and hyperpolarizability, respectively, and $\sigma'_{\alpha\beta,\gamma\delta}$ and $\sigma''_{\alpha\beta,\gamma\delta,\epsilon\sigma}$ are components of the quadrupole shielding polarizability and hyperpolarizability, respectively. Dipole shielding (hyper)polarizabilities have been calculated for the water molecule[13–17] but the corresponding quadrupole

 0021-9606/97/106(20)/8332/7/$10.00

shielding polarizabilities have only been estimated for a few molecules.[11–13,18] For the water molecule, only a rotationally averaged value of one of the components has been presented.[13] In our previous work,[10] we truncated the above series after the second term, thus calculating the electrostatic interaction term as

$$\langle \sigma_{E,\alpha\beta} \rangle = \sigma'_{\alpha\beta,\gamma} \langle E_\gamma \rangle + \frac{1}{2} \sigma''_{\alpha\beta,\gamma\delta} \langle E_\gamma E_\delta \rangle, \tag{2}$$

where brackets denote ensemble averages obtained from molecular dynamics simulations. We used the shielding (hyper)-polarizabilities calculated by Rizzo *et al.*[17] Here, we also include the linear field-gradient term and the electrostatic term is thus given as

$$\langle \sigma_{E,\alpha\beta} \rangle = \sigma'_{\alpha\beta,\gamma} \langle E_\gamma \rangle + \frac{1}{2} \sigma''_{\alpha\beta,\gamma,\delta} \langle E_\gamma E_\delta \rangle + \sigma'_{\alpha\beta,\gamma\delta} \langle E_{\gamma\delta} \rangle. \tag{3}$$

In addition to our previous work,[10] we thus also have to calculate the quadrupole shielding polarizabilities, $\sigma'_{\alpha\beta,\gamma\delta}$, and the field gradient, $\langle E_{\gamma\delta} \rangle$. The quadrupole shielding polarizabilities are determined from quantum chemical calculations of the shielding tensors of a single water molecule under the influence of point charges and dipoles. The procedure is described in section II. The simulations of the electric field-gradients are presented in section III and the chemical shifts are discussed in section IV. Finally, we conclude our work in section V.

II. CALCULATION OF QUADRUPOLE SHIELDING POLARIZABILITIES

The quadrupole shielding polarizabilites, $\sigma'_{\alpha\beta,\gamma\delta}$, have been calculated from quantum chemical *ab initio* calculations. A component of the shielding tensor in a water molecule interacting with a set of charges, i, is the sum of the shielding tensor of water in vacuum, $\sigma^0_{\alpha\beta}$, and a difference tensor, i.e.,

$$\sigma^i_{\alpha\beta} = \sigma^0_{\alpha\beta} + \Delta\sigma^i_{\alpha\beta}, \tag{4}$$

where the difference tensor, $\Delta\sigma^i_{\alpha\beta}$, in the usual perturbative fashion is given as

$$\Delta\sigma^i_{\alpha\beta} = \sigma'_{\alpha\beta,\gamma} E^i_\gamma + \frac{1}{2} \sigma''_{\alpha\beta,\gamma,\delta} E^i_\gamma E^i_\delta + \sigma'_{\alpha\beta,\gamma\delta} E^i_{\gamma\delta}, \tag{5}$$

since we assume that the electrostatic interactions alone are responsible for the change in the shielding tensor. Here $\sigma'_{\alpha\beta,\gamma}$, $\sigma''_{\alpha\beta,\gamma,\delta}$ and $\sigma'_{\alpha\beta,\gamma\delta}$ are to be considered as parameters and can thus be obtained from least squares fitting to the set $\{\Delta\sigma^i_{\alpha\beta}, E^i_\gamma, E^i_{\gamma\delta}\}$. A fitting procedure is performed for each tensor element. We have used a singular value decomposition (SVD) approach,[19] since the parameters are not guaranteed to be linearly independent. By symmetry the number of required fits is reduced to 3 for both oxygen and hydrogen. The number of parameters in each fit is reduced to 7 and 9 for oxygen and hydrogen, respectively, also by symmetry.

TABLE I. Geometries for the water molecule.

Geometry	Parameters	
	r_{OH}/Å	α/deg.
NEMO[a]	0.958	104.5
Liquid[b]	0.951	110.2

[a]See Ref. 7.
[b]See Ref. 22.

When choosing the set of charge distributions we restrict ourselves to distributions resembling the charge distribution in liquid water, since our goal is to model $\Delta\sigma_{\alpha\beta}$ accurately for this particular charge distribution. We also ensure that the charge closest to the water molecule is negative in order to minimize charge transfer effects. Other applications of this *point charge method* can be found in, e.g., Refs. 12, 20, and 21.

We have estimated parameters for two different geometries; an experimental gas-phase geometry which is the one used in the NEMO potential (from now referred to as the NEMO-geometry) and a liquid phase geometry calculated theoretically by Moriarty and Karlström[22] in a combined quantum chemical and statistical mechanical approach (referred to as the liquid geometry). The geometries are given in Table I. We have carried out calculations of the hydrogen and oxygen parameters for both geometries at the Hartree-Fock (HF) level. The oxygen parameters have also been calculated at the MCSCF level using a Complete Active Space Self-Consistent Field (CASSCF) method for the NEMO-geometry. The chosen CAS space is (6331). We have used the Dalton program[23] and the atomic natural orbital (ANO) basis sets by Widmark *et al.*[24] We have previously[10] examined the basis set convergence of nuclear shieldings of the water dimer at the HF level. From these calculations we conclude that the contracted basis set ANO$[5s4p3d2f/4s3p2d]$ is sufficiently accurate. We also calculate the mean shielding polarizability tensors which are defined as

$$A_\beta = -\frac{1}{3} \sigma'_{\alpha\alpha,\beta} \tag{6}$$

and

$$B_{\beta\beta} = -\frac{1}{6} \sigma''_{\alpha\alpha,\beta,\beta}, \tag{7}$$

and the mean quadrupole shielding polarizability tensor,

$$C_{\beta\beta} = \frac{1}{3} \sigma'_{\alpha\alpha,\beta\beta}, \tag{8}$$

where we have used the Einstein summation convention.

The dipole shielding (hyper)polarizabilities found by the point-charge method described above are given in Table II for oxygen. The parameters are given for both the NEMO and the liquid geometry at the HF level and for the NEMO geometry at the CAS level.

TABLE II. Shielding polarizabilities and hyperpolarizabilities for oxygen.

Parameter	Geometry/method NEMO/HF	Liquid/HF	NEMO/CAS
A_z	−396.6	−359.4	−295.3
B_{xx}	−13686	−14018	−13337
B_{yy}	12533	12288	11737
B_{zz}	1201	1071	838
$\sigma'_{xx,z}$	500.8	458.8	436.9
$\sigma'_{yy,z}$	360.3	352.9	263.4
$\sigma'_{zz,z}$	328.6	266.4	185.6
$\sigma''_{xx,x,x}$	17752	17406	19668
$\sigma''_{xx,y,y}$	−19721	−18791	−19505
$\sigma''_{xx,z,z}$	−8369	−8038	−7705
$\sigma''_{yy,x,x}$	30583	33414	27646
$\sigma''_{yy,y,y}$	−20795	−21985	−18037
$\sigma''_{yy,z,z}$	645.3	826.1	1168
$\sigma''_{zz,x,x}$	33778	33285	32711
$\sigma''_{zz,y,y}$	−34679	−32951	−32880
$\sigma''_{zz,z,z}$	519.1	788.8	1508

TABLE III. Quadrupole shielding polarizabilities for oxygen.

Parameter	Geometry/method NEMO/HF	Liquid/HF	NEMO/CAS
C_{xx}	−334.0	−330.0	−320.1
C_{yy}	92.6	113.3	129.1
C_{zz}	241.5	216.7	191.0
$\sigma'_{xx,xx}$	−136.6	−116.2	−144.2
$\sigma'_{xx,yy}$	−108.6	−92.0	−60.1
$\sigma'_{xx,zz}$	245.2	208.1	204.2
$\sigma'_{yy,xx}$	−482.8	−517.5	−434.1
$\sigma'_{yy,yy}$	237.3	266.5	224.2
$\sigma'_{yy,zz}$	245.6	251.0	210.0
$\sigma'_{zz,xx}$	−382.7	−356.4	−382.1
$\sigma'_{zz,yy}$	149.1	165.3	223.3
$\sigma'_{zz,zz}$	233.7	191.1	158.8

Considering first the shielding polarizabilities, it is noted that the parameters obtained for the different geometries at the HF level are similar, and larger than the CAS values. This overestimation of the linear field effect at the HF level has also been observed elsewhere.[17] Although the HF parameters are similar, we note that the polarizabilities are larger for the NEMO geometry as compared to the liquid geometry, indicating a quite strong geometry dependence of the shielding polarizabilities, which has previously been noted by Rizzo *et al.*[17]

When we consider the oxygen shielding hyperpolarizabilities, the picture is different. The deviations between the HF and the CAS numbers are smaller, but the differences are larger for parameters $\sigma''_{\alpha\alpha,z,z}$, the main difference being the large CAS result for $\sigma''_{zz,z,z}$. When comparing the shielding hyperpolarizabilities with the results obtained in Ref. 17, the differences are substantial for parameters $\sigma''_{\alpha\alpha,x,x}$ and $\sigma''_{\alpha\alpha,y,y}$ but we note a much better agreement for parameters $\sigma''_{\alpha\alpha,z,z}$; in Ref. 17 CAS values are obtained for B_{xx}, B_{yy} and B_{zz} of 2125.2, −800.0 and 1367.6 (ppm a.u.), respectively. We also note that $\sigma''_{\alpha\alpha,x,x}$ and $\sigma''_{\alpha\alpha,y,y}$ are much larger than $\sigma''_{\alpha\alpha,z,z}$. The difference in the agreement of the components arises from the use of different procedures. Rizzo *et al.* apply a finite-field approach,[17] whereas we bias our calculation towards electric field components that are important in liquid water. The electric field at the oxygen atom in liquid water is zero along the x and y axes by symmetry. Thus, mostly charge distributions consisting of point charges and dipoles along the z axis have been considered for calculating the oxygen parameters, and we therefore get a poorer description of parameters $\sigma''_{\alpha\alpha,x,x}$ and $\sigma''_{\alpha\alpha,y,y}$. This will not affect the chemical shieldings since the corresponding squared field components $\langle E_x E_x \rangle$ and $\langle E_y E_y \rangle$ are almost zero in liquid water.[10]

The quadrupole shielding parameters for oxygen are given in Table III. We again note some geometry dependence and the differences between the HF and the CAS numbers are comparable to the dipole shielding polarizability differences. We note that both C_{xx} and C_{yy} are increased while C_{zz} is decreased while going from HF to CAS. In Ref. 13 the value of C_{zz} is computed to 190.8 ppm/a.u. at the Hartree-Fock level which is in reasonable agreement with our values.

In Figure 1 we demonstrate the quality of the fit by showing the diagonal tensor elements of the difference tensor, $\Delta\sigma^i_{\alpha\alpha}$, for calculations where the water molecule interacts with a point charge of -1 a.u. at $(0,0,-z)$, as a function of z, using the NEMO geometry at the HF level. In the calculations, the oxygen atom is placed at the origin and the hydrogen atoms are placed at $(\pm x,0,z)$. In this work we have neglected overlap effects. It is observed, that the intermolecular shielding function for the argon dimer [i.e., $\sigma(r_{Ar-Ar})$] resembles the intermolecular potential, although with a minima at a much shorter interatomic separation than the potential minima.[25] For intermolecular separations close

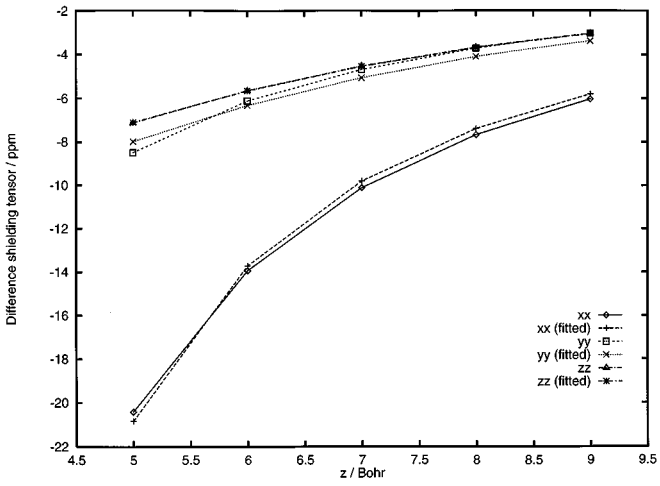

FIG. 1. The diagonal elements of the oxygen shielding tensor in a water molecule (NEMO geometry) interacting with a negative point charge at $(0,0,-z)$.

TABLE IV. Shielding polarizabilities and hyperpolarizabilities for hydrogen.

	Geometry/method	
Parameter	NEMO/HF	Liquid/HF
A_x	70.7	70.7
A_z	43.2	38.3
B_{xx}	102.4	49.1
B_{yy}	110.6	147.2
B_{zz}	170.9	142.3
B_{xz}	−529.5	−424.2
$\sigma'_{xx,x}$	−46.2	−46.5
$\sigma'_{xx,z}$	−50.4	−44.2
$\sigma'_{yy,x}$	−78.7	−79.4
$\sigma'_{yy,z}$	−53.7	−48.0
$\sigma'_{zz,x}$	−87.1	−86.1
$\sigma'_{zz,z}$	−25.5	−22.7
$\sigma''_{xx,x,x}$	−287.0	−202.2
$\sigma''_{xx,y,y}$	−207.6	−259.9
$\sigma''_{xx,z,z}$	−347.3	−324.3
$\sigma''_{xx,x,z}$	518.3	431.4
$\sigma''_{yy,x,x}$	−120.1	−63.3
$\sigma''_{yy,y,y}$	−90.6	−153.4
$\sigma''_{yy,z,z}$	−347.9	−298.7
$\sigma''_{yy,x,z}$	522.6	454.0
$\sigma''_{zz,x,x}$	−207.2	−28.8
$\sigma''_{zz,y,y}$	−365.3	−469.7
$\sigma''_{zz,z,z}$	−329.9	−231.0
$\sigma''_{zz,x,z}$	547.5	387.1

to (and less than) this shielding function minima, overlap effects are of course significant. The fact that the curves in Figure 1 do not contain any ''repulsive'' overlap contribution indicates that overlap effects are small, at least in the case of the interaction between water and a point charge. It is thus noted that we have included points where effects arising from placing the point charges within the charge distribution of the water molecule are negligible.

The obtained shielding (hyper)polarizabilities for hydrogen are given in Table IV. These parameters were calculated for the two geometries at the HF level. We note that the shielding polarizabilities are quite similar for the two geometries. The main difference is the change in A_z when going from the NEMO to the liquid geometry.

When the shielding hyperpolarizabilities for the two geometries are compared, the parameters look very different; B_{xx} is for example decreased by 50% when going from the NEMO to the liquid geometry. However, note that while B_{xx} and B_{zz} decrease when going from NEMO to liquid, B_{xz} increase significantly (we do not take B_{yy} into account, since $\langle E_y E_y \rangle$ is close to zero in liquid water[10]). It is thus difficult to determine whether the shielding hyperpolarizability contribution to the shift is altered by examining the parameters alone. It should also be noted that the three parameters $\sigma''_{\alpha\alpha,x,x}$, $\sigma''_{\alpha\alpha,z,z}$ and $\sigma''_{\alpha\alpha,x,z}$ are not independent. The hydrogen quadrupole shielding polarizabilities are given in Table V. These are very similar for the two geometries. We further note that C_{yy} is small.

TABLE V. Quadrupole shielding polarizabilities for hydrogen.

	Geometry/method	
Parameter	NEMO/HF	Liquid/HF
C_{xx}	13.7	14.4
C_{yy}	−1.1	0.2
C_{zz}	−12.4	−14.6
C_{xz}	36.9	33.9
$\sigma'_{xx,xx}$	10.4	12.4
$\sigma'_{xx,yy}$	−0.2	0.1
$\sigma'_{xx,zz}$	−10.1	−12.4
$\sigma'_{xx,xz}$	38.0	34.8
$\sigma'_{yy,xx}$	12.1	14.1
$\sigma'_{yy,yy}$	−7.1	−6.2
$\sigma'_{yy,zz}$	−4.8	−7.8
$\sigma'_{yy,xz}$	36.3	32.6
$\sigma'_{zz,xx}$	18.5	16.7
$\sigma'_{zz,yy}$	3.9	6.9
$\sigma'_{zz,zz}$	−22.4	−23.5
$\sigma'_{zz,xz}$	36.3	34.4

III. MOLECULAR DYNAMICS SIMULATIONS

The molecular dynamics simulations have been carried out with the MOLSIM program.[26] We have used the NEMO potential[7] with the extension to atomic dipole moments and atomic polarizability tensors.[27] The simulated system consists of 216 water molecules enclosed in a cubic box. In the calculation of the forces, periodic boundary conditions have been adopted with a spherical cut-off of 8.5 Å. The induced dipole moments have been calculated by a first-order predictor, but a full iterative solution has been carried out every fifth time step in order to avoid drifting.[28] The NVT-ensemble was employed by scaling the velocities to the appropriate temperature.[29] The equations of motion of the rigid molecules were integrated by using quaternions[30] and the velocity Verlet algorithm[31] using a timestep of 2.0 fs. We have carried out simulations of 110 ps including 10 ps of equilibration at four different temperatures (269, 300, 338 and 448 K) at experimental densities. The water molecule has been placed in the xz-plane with the z axis as the C_2 axis. We consider properties of the hydrogen atom situated at $(+x,0,+z)$.

The ensemble averages of the electric fields at the oxygen and hydrogen atoms have been calculated previously,[10] and ensemble averages of the electric field gradient are given as a function of temperature in Tables VI and VII for oxygen

TABLE VI. Electric field-gradient components (in 10^{-3} atomic units) at the oxygen nuclei of the water molecule.

T/K	$\langle E_{xx} \rangle$	$\langle E_{yy} \rangle$	$\langle E_{zz} \rangle$
269	23.3	−17.2	−6.1
300	20.7	−14.8	−5.9
338	18.2	−12.7	−5.5
448	12.7	−8.5	-4.2

TABLE VII. Electric field-gradient components (in 10^{-3} atomic units) at the hydrogen nuclei of the water molecule.

T/K	$\langle E_{xx} \rangle$	$\langle E_{yy} \rangle$	$\langle E_{zz} \rangle$	$\langle E_{xz} \rangle$
269	20.3	−14.1	−6.2	10.2
300	18.5	−12.7	−5.8	9.0
338	16.6	−11.3	−5.3	7.7
448	12.2	−8.2	−4.0	5.0

and hydrogen. We only give the non-vanishing components. It is noted that all components decrease with increasing temperature, as also noted for the electric fields.[10] Figure 2 shows the distribution of the oxygen field gradient as a function of temperature, and Figure 3 shows the same for hydrogen. The oxygen components may for the three lowest temperatures be fitted to Gaussian functions, but this is not the case for the hydrogen components. Especially the distribution of the *xz* component at 338 K is broad with a shape very different from a Gaussian distribution. The field gradient distribution is thus more complex than the field distribution, which can be described by Gaussian functions for the electric fields at both the oxygen and hydrogen nuclei.[10]

IV. CHEMICAL SHIFTS

For the electric field contribution to the oxygen shift (Table VIII), we note that when shifting the geometry from NEMO to liquid, it is lowered by about 1.5 ppm, which is mainly due to the change in the first order contribution. When going from the HF to the CAS level of accuracy, the total shift is lowered by about 4 ppm (the linear part is lowered by about 5 ppm). In comparison with our previous work,[10] the field effect is lowered with about 2 ppm for our most accurate value, NEMO/CAS. If the liquid geometry is applied, the shift is furthermore lowered by 1–2 ppm.

For hydrogen (Table IX), we find very similar results for the NEMO and the liquid geometry. The largest difference is about 0.2 ppm. This is to be expected from the good agreement of the dipole shielding polarizability parameters of hydrogen.

The electric field-gradient effects on the shieldings are given in Table X. It is about −10 ppm for the oxygen shift and about 0.7 ppm for the proton shift, and it is almost independent of geometry. For oxygen, the results obtained from CAS and HF calculations are also very much alike. It is also noted that its temperature dependence is substantial and opposes the temperature dependence of the linear electric field contribution. This contribution is thus large for oxygen and also significant for hydrogen.

The total gas-to-liquid shifts of water are given in Table XI. The numbers are obtained from adding the field and the field-gradient effect calculated here to the van der Waals effect obtained in Ref. 10. We use the NEMO/CAS numbers for oxygen and the NEMO/HF numbers for hydrogen. We note that the total oxygen shift is changed, compared to our previous work,[10] by about −12 ppm at room temperature of which about −10 ppm is the field-gradient effect and the rest originates from the geometry dependence of the dipole

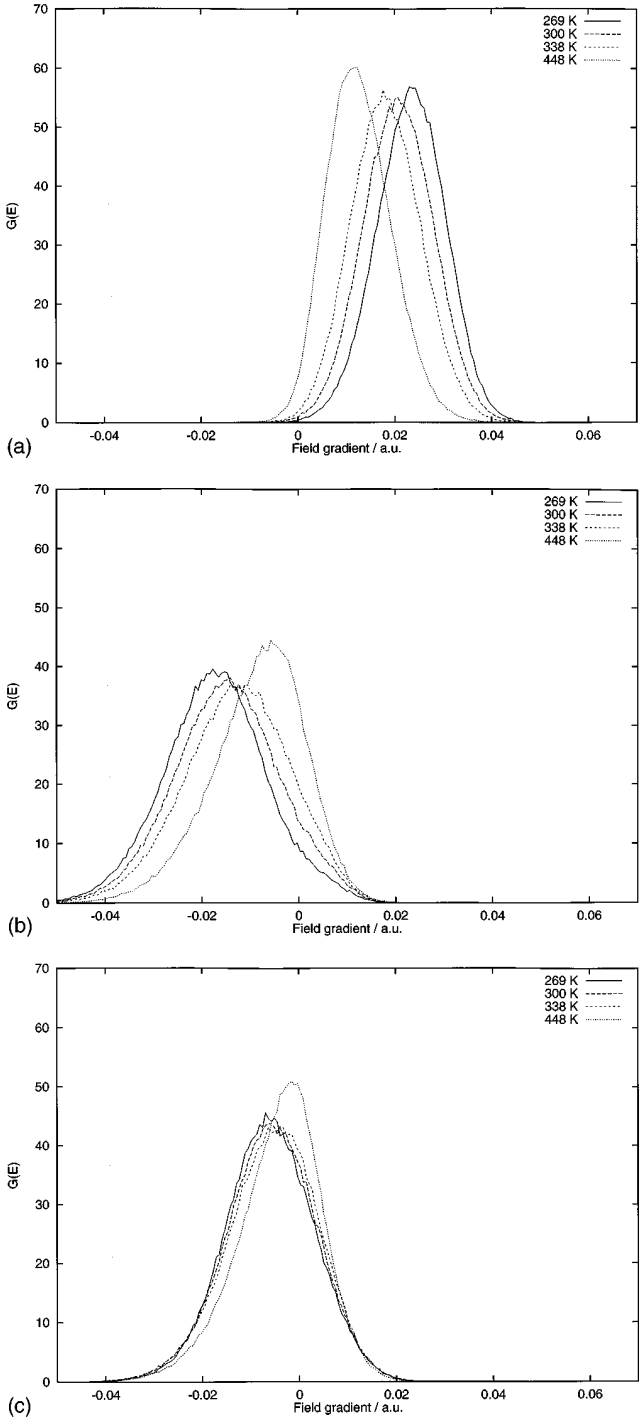

FIG. 2. Electric field-gradient distributions at the oxygen atom. (a) The *xx* component. (b) The *yy* component. (c) The *zz* component.

shielding (hyper)polarizabilities. The inclusion of the field-gradient effect on the oxygen shielding thus brings us substantially closer to the experimental value.[32] However, even if a pure (intramolecular) geometrical contribution of −10 to −5 ppm[10] is added, we are still about 20 ppm from the experimental value of −36 ppm at room temperature.[32] In contrast to our previous work,[10] we now describe the temperature dependence qualitatively correct, even though it is smaller than in the experiment.[32]

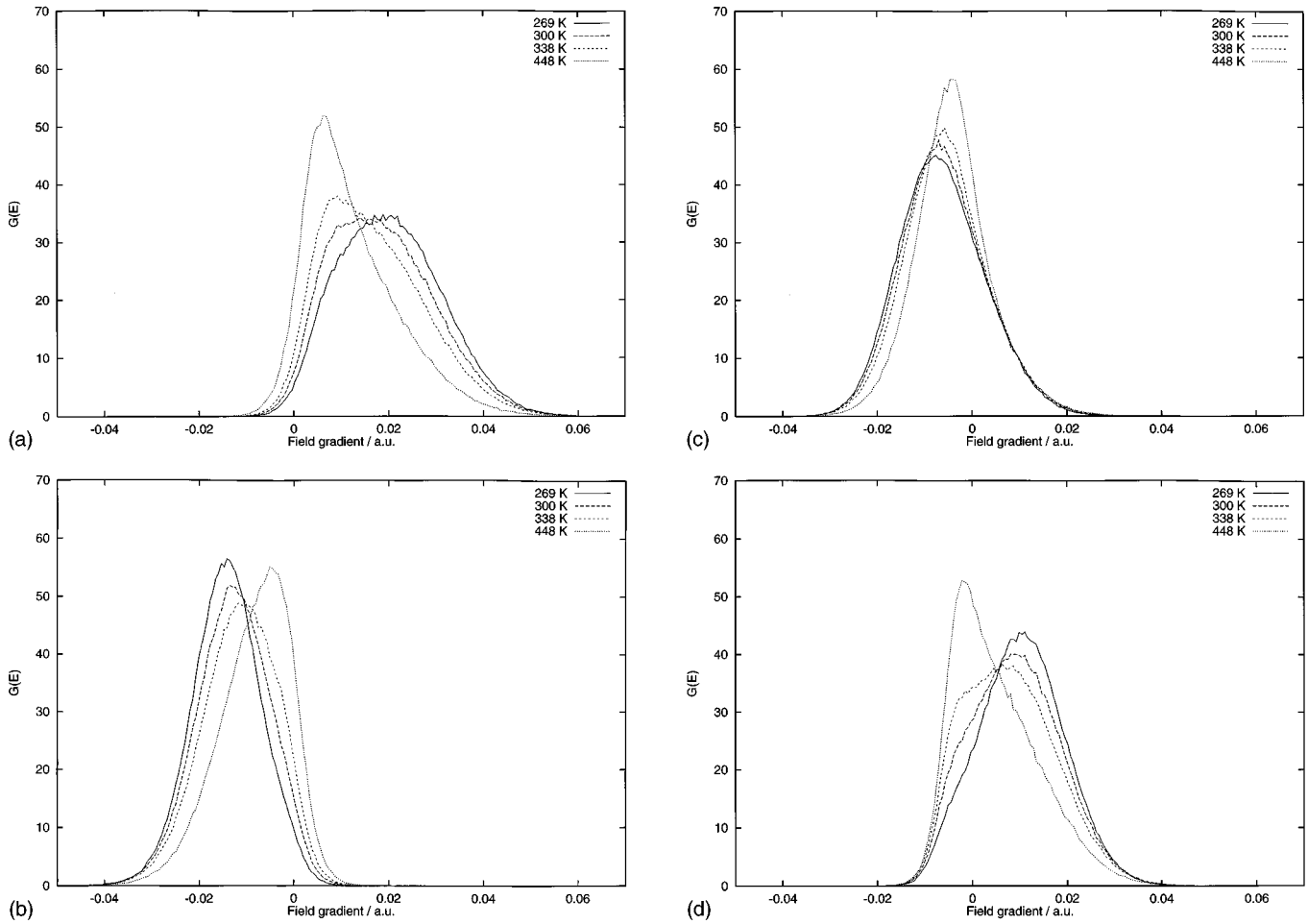

FIG. 3. Electric field-gradient distributions at the hydrogen atom. (a) The *xx* component. (b) The *yy* component. (c) The *zz* component. (d) The *xz* component.

TABLE VIII. Electric field effects on oxygen shielding (in ppm) for different geometries and quantum chemical methods.

	NEMO/HF		
T/K	1st order	2nd order	Total
269	20.97	−4.99	15.98
300	19.46	−4.52	14.94
338	17.84	−4.01	13.84
448	13.92	−2.73	11.19
	Liquid/HF		
269	19.01	−4.52	14.49
300	17.64	−4.10	13.54
338	16.17	−3.64	12.53
448	12.62	−2.47	10.14
	NEMO/CAS		
269	15.62	−3.78	11.83
300	14.49	−3.45	11.05
338	13.29	−3.08	10.21
448	10.37	−2.11	8.25

The total proton shift is changed by about 0.8 ppm. This result (−3.04 ppm) is comparable to the result obtained in Ref. 6 of −3.2 ppm by calculating the shielding of the center molecule in a set of clusters generated by molecular dynamics simulations. It was, however, noted in our previous work that the geometrical effect is about −1.5 to −0.7 ppm, which

TABLE IX. Electric field effects on hydrogen shielding (in ppm).

	Geometry/method		
	NEMO/HF		
T/K	1st order	2nd order	Total
269	−4.28	0.30	−3.98
300	−3.94	0.24	−3.69
338	−3.57	0.19	−3.38
448	−2.71	0.10	−2.62
	Liquid/HF		
269	−4.05	0.25	−3.80
300	−3.72	0.21	−3.51
338	−3.37	0.17	−3.21
448	−2.55	0.08	−2.48

TABLE X. Electric field gradient effects on shielding (in ppm).

	Oxygen			Hydrogen	
T/K	NEMO/HF	Liquid/HF	NEMO/CAS	NEMO/HF	Liquid/HF
269	−10.86	−10.97	−10.85	0.75	0.73
300	−9.73	−9.81	−9.68	0.67	0.65
338	−8.59	−8.64	−8.52	0.59	0.57
448	−6.05	−6.08	−5.98	0.41	0.40

may explain the difference with respect to experiment.[33] It is furthermore noted that the temperature dependence is qualitatively modelled, even though the temperature dependence is stronger in the experiment.[33]

Effects arising from the change in molecular geometry on the nuclear shieldings of liquid water can be partioned into (at least) four parts: an intramolecular part, which has been discussed in our previous work,[10] a polarizability term arising from the geometry dependence of especially the dipole shielding polarizabilities, a term arising from the change in the electrostatics of the liquid when the geometry is changed and finally a contribution from the difference in the zero-point vibrational contribution. Neither of these four terms are formally included here. Our previous work[10] shows that the first term contributes down to −1.5 ppm to the hydrogen shift and −10 ppm to the oxygen shift. The results given here, indicate that the second term is negligible for the hydrogen shift and contributes about −2 ppm to the oxygen shift. Furthermore, zero-point vibrational contributions may be substantial, since the rovibrational contribution to the gas phase water shieldings is large[34] and the potential energy surfaces of water differ in the liquid and the gas phase.[22]

Other effects that may be substantial for the oxygen shift are overlap effects[25,35–39] and contributions from the magnetizability anisotropy of the surrounding molecules.[2] Magnetizability anisotropy effects should, however, affect the proton shielding to the same extent as the oxygen shielding.

V. CONCLUSIONS

We have calculated the contributions to the gas-to-liquid chemical shift of water arising from the intermolecular field gradient in addition to the electric field effect. This contribution is large for the oxygen shift and cannot be neglected for the proton shift. The oxygen shielding is shifted 10 ppm towards the experiment,[32] whereas the proton shielding is shifted about 0.7 ppm. The proton shifts are still in good agreement with experiment.[33] For the oxygen shift, the discrepancies between theory and experiment are still substantial, even if this work presents a considerable improvement.

TABLE XI. Solvent effects to nuclear shielding (in ppm).

	Oxygen		Hydrogen	
T/K	Calculated	Experimental	Calculated	Experimental
269	−7.91	⋯	−3.20	−4.70
300	−7.39	−36	−3.04	−4.35
338	−6.66	⋯	−2.86	−4.02
448	−4.80	−27	−2.37	⋯

ACKNOWLEDGMENT

Grants from the Danish Natural Research Council (SNF) are gratefully acknowledged.

[1] M. J. Stephen, Mol. Phys. **1**, 223 (1958).
[2] A. D. Buckingham, T. Schaefer, and W. G. Schneider, J. Chem. Phys. **32**, 1227 (1960).
[3] A. D. Buckingham, Can. J. Chem. **38**, 300 (1960).
[4] A. D. Buckingham, Adv. Chem. Phys. **12**, 107 (1967).
[5] D. B. Chesnut and B. E. Rusiloski, J. Mol. Struct. (Theochem) **314**, 19 (1994).
[6] V. G. Malkin, O. L. Malkina, G. Steinebrunner, and H. Huber, Chem. Eur. J. **2**, 452 (1996).
[7] A. Wallqvist and G. Karlström, Chem. Scr. **29A**, 131 (1989).
[8] P.-O. Åstrand, A. Wallqvist, G. Karlström, and P. Linse, J. Chem. Phys. **95**, 8419 (1991).
[9] P.-O. Åstrand, A. Wallqvist, and G. Karlström, J. Chem. Phys. **100**, 1262 (1994).
[10] T. Nymand, P.-O. Åstrand, and K. V. Mikkelsen, J. Phys. Chem. (in press).
[11] J. G. Batchelor, J. Am. Chem. Soc. **97**, 3410 (1975).
[12] J. D. Augspurger, C. E. Dykstra, and E. Oldfield, J. Am. Chem. Soc. **113**, 2447 (1991).
[13] J. D. Augspurger and C. E. Dykstra, J. Phys. Chem. **95**, 9230 (1991).
[14] M. Grayson and W. T. Raynes, Chem. Phys. Lett. **214**, 473 (1993).
[15] M. Grayson and W. T. Raynes, Chem. Phys. Lett. **218**, 270 (1994).
[16] M. Grayson and W. T. Raynes, Chem. Phys. Lett. **224**, 602 (1994).
[17] A. Rizzo, T. Helgaker, K. Ruud, A. Barszczewicz, M. Jaszuński, and P. Jørgensen, J. Chem. Phys. **102**, 8953 (1995).
[18] J. Augspurger, J. G. Pearson, E. Oldfield, C. E. Dykstra, K. D. Park, and D. Schwartz, J. Magn. Res. **100**, 342 (1992).
[19] W. H. Press, S. A. Teukolsky, W. T. Vetterling, and B. P. Flannery, *Numerical Recipes* (Cambridge U.P., Cambridge, 1992).
[20] J. D. Augspurger and C. E. Dykstra, J. Am. Chem. Soc. **115**, 12 016 (1993).
[21] P.-O. Åstrand and G. Karlström, Mol. Phys. **77**, 143 (1992).
[22] N. W. Moriarty and G. Karlström, J. Chem. Phys. **106**, 6470 (1997).
[23] T. Helgaker, H. J. Aa. Jensen, P. Jørgensen, J. Olsen, H. Ågren, T. Andersen, K. L. Bak, V. Bakken, O. Christiansen, P. Dahle, E. K. Dalskov, T. Enevoldsen, B. Fernandez, H. Heiberg, H. Hettema, D. Jonsson, S. Kirpekar, R. Kobayashi, H. Koch, K. V. Mikkelsen, P. Norman, M. J. Packer, K. Ruud, T. Saue, P. R. Taylor, and O. Vahtras, Dalton, an *ab initio* electronic structure program. See the DALTON manual at http://www.kjemi.uio.no/software/dalton/dalton.html .
[24] P.-O. Widmark, P.-A. Malmqvist, and B. O. Roos, Theor. Chim. Acta **77**, 291 (1990).
[25] C. J. Jameson and A. C. de Dios, J. Chem. Phys. **97**, 417 (1992).
[26] P. Linse and A. Wallqvist, *MOLSIM 1.2*, Lund University, Sweden, 1991.
[27] P.-O. Åstrand, P. Linse, and G. Karlström, Chem. Phys. **191**, 195 (1995).
[28] P. Ahlström, A. Wallqvist, S. Engström, and B. Jönsson, Mol. Phys. **68**, 563 (1989).
[29] H. J. C. Berendsen, J. P. M. Postma, W. F. van Gunsteren, A. DiNola, and J. R. Haak, J. Chem. Phys. **81**, 3684 (1984).
[30] M. P. Allen and D. S. Tildesley, *Computer Simulations of Liquids* (Clarendon, Oxford, 1987).
[31] W. C. Swope, H. C. Andersen, P. H. Berens, and K. R. Wilson, J. Chem. Phys. **76**, 637 (1982).
[32] A. E. Florin and M. Alei, J. Chem. Phys. **47**, 4268 (1967).
[33] J. C. Hindman, J. Chem. Phys. **44**, 4582 (1966).
[34] P. W. Fowler and W. T. Raynes, Mol. Phys. **43**, 65 (1981).
[35] A. D. Buckingham and K. P. Lawley, Mol. Phys. **3**, 219 (1960).
[36] C. J. Jameson and A. C. de Dios, J. Chem. Phys. **98**, 2208 (1993).
[37] C. J. Jameson and H. M. Lim, J. Chem. Phys. **103**, 3885 (1995).
[38] A. Freitag, C. van Wüllen, and V. Staemmler, Chem. Phys. **192**, 267 (1995).
[39] A. Barszczewicz, M. Jaszuński, T. Helgaker, and K. Ruud, Chem. Phys. Lett. **250**, 1 (1996).